

FIG. 10. Plot of DDB using the prenormalized curves from Fig. 9 [$\Delta n'(t) = \Delta n(t)/\Delta n$ (4 μsec)]. The filled circles have been obtained by subjecting the primary difference curve to a 3-point averaging procedure. The dashed lines represent expected difference curves for various values of R ($= \tau_{\text{XHR}}/\tau_{\text{KP}} - 1$) as indicated. The solid line represents a least-squares best fit to the experimental difference curve ($R = 0.24 \pm 0.01$).

tour length and persistence length, P , to the decay time that same polymer would have if it were a perfectly straight, rigid rod. The ratio, $\tau(P)/\tau(\text{Rod})$, is given by

$$R_c = \tau(P)/\tau(\text{Rod}) = R_a X(1 - Y) \quad (6)$$

where

$$R_a = 1.012 - 0.248X + 0.0337X^2 - 0.00198X^3$$

$$Y = 0.0647X - 0.0115X^2 + 0.000989X^3$$

and where X is the contour length of the polymer in units of P . The range of validity of Eq. (6) is given by

$$0.1 < X < 5.0; \quad L/d > 20.$$

For DNA, this corresponds to molecules ranging in size from 150 bp to about 730 bp (for $P = 500 \text{ \AA}$).⁹ [For further discussions regarding the application of Eq. (6), see Refs. 3,9,13.]

Equation (6) has been used to determine the value of P for DNA directly.⁹ However, it can also be used in association with a DDB analysis

to provide a correction for residual flexibility. In this latter instance, $R_{c,1}/R_{c,2}$ can be used even if $L/d < 20$, since attendant errors will be quite small as that ratio approaches unity.

It should be noted that the assumption of "rod-like" character (i.e., structural rigidity) for flexible polymers shorter than one persistence length is rendered invalid by the extreme sensitivity of TEB. For example, a DNA molecule 100 bp long ($X = 0.68$ for $P = 500 \text{ \AA}$) would demonstrate a birefringence decay time approximately 18% below that expected for the rigid-rod limit. Therefore, in determining various structural features for DNA, as well as for other flexible polymers, one needs to make appropriate corrections for residual flexibility. For the 100-bp DNA molecule referred to above, failure to account for residual flexibility would lead to an apparent rise/bp of only 3.2 \AA (assuming that the true rise/bp is 3.4 \AA).

[14] Measurements of Protein Hydration by Various Techniques

By HELMUT PESSEN and THOMAS F. KUMOSINSKI

Introduction

The problems of measuring the interaction of water with biological macromolecules have long plagued biochemists. The importance of this interaction with respect to protein primary, secondary, and tertiary structure is well documented.¹ Nevertheless, several basic aspects of this topic remain unresolved. Among these are a clear definition of the hydration of a protein, an understanding of the relationships between different experimental values of total hydration and the methods of measurement from which they are obtained, and whether the interactions are strong or weak.

In this chapter we will deal with hydration measurements made on globular proteins in solution² by three techniques which have been found in recent years to afford certain useful insights: nuclear magnetic resonance (NMR) relaxation, small-angle X-ray scattering (SAXS), and hydrodynamics (velocity sedimentation). The latter two will be treated together, because sedimentation, which cannot by itself give definitive

¹ I. D. Kuntz and W. Kauzmann, *Adv. Protein Chem.* **28**, 239 (1974).

² The study of hydration by NMR measurements of nonfreezable water does not fall within the purview of this article. It has been reviewed elsewhere.¹

values of hydration, is very useful in corroborating SAXS data. Conversely, sedimentation coefficients can be calculated independently from SAXS. NMR methodology will be treated in particular detail, both because of its potential utility for the present purpose, and because previous treatment in the literature has been somewhat limited. Specific discussions of these methods will be followed by some general remarks, including an evaluation of the different approaches.

Approaches

NMR Relaxation

Theory. Proteins, by their very nature as polyelectrolytes with large charge-to-mass ratios, are susceptible to severe interaction effects in solution. Although the consequent deviations from ideality are among the most important effects in solution theory, they have not received sufficient consideration in NMR studies of proteins. A prime example is the nonideality caused by repulsion due to net positive or negative charges, which has been demonstrated to have serious effects on measurements other than NMR (light scattering, osmotic pressure, sedimentation equilibrium and velocity, translational diffusion, and even pH titration).^{1,3-7} Thus Pedersen,⁵ on the basis of the theory of Tiselius,⁶ as early as 1940 showed that a potential gradient is created in a sedimenting solution during both equilibrium and velocity runs as a result of high net charge on a macromolecule; Booth⁷ has quantitated such behavior by a general theory for charged spheres. Sedimentation coefficients of bovine serum albumin at acid pH are lower by at least half when compared with the same protein in the presence of 0.1 M salt⁸; the salt thus minimizes the high repulsive effect of the molecular charges. Light scattering and osmotic pressure measurements of aqueous proteins carrying high net charge indicate decreased apparent weight-average molecular weights with increasing concentration, in consequence of intermolecular repulsion,^{3,9-11} according to the equation:

$$M_{w,app}^{-1} = M_{w,0}^{-1} (1 + cd \ln \gamma/dc)$$

where γ is the activity coefficient of the protein at a concentration c , $M_{w,app}$ is the experimentally derived apparent weight-average molecular weight, and $M_{w,0}$ is the true molecular weight at infinite dilution of the protein. From the virial expansion for osmotic pressure it follows that

$$d \ln \gamma/dc = 2B_0 + 3B_1c + \dots$$

where the B quantities are the second and higher virial coefficients; for repulsive effect usually $d \ln \gamma/dc = 2B_0 > 0$ (i.e., $\gamma > 1$), in accord with general electrolyte solution theory.

Beyond simple electrostatic repulsion, one needs to be concerned with a less obvious phenomenon, namely the charge fluctuations treated in the theory of Kirkwood and Shumaker.¹² Extensive experimental evidence for this theory has been furnished by many investigations using light scattering; for proteins in water under isoionic conditions the apparent weight-average molecular weight increases with increasing concentration.¹³⁻¹⁶ Ordinarily, this phenomenon might be interpreted simply as an aggregation of the molecule. However, Kirkwood and Shumaker have shown that, since proteins are polyampholytes rather than simple polyelectrolytes, attractive forces arise in isoionic protein solutions from statistical fluctuations, both in charge and in charge distribution; these in turn are associated with fluctuations in the number and configurations of protons bound to the protein molecule. Briefly stated, one or more virial coefficients in $c^{n/2}$ powers must be added to Eq. (2) and these coefficients due to progressive ionization of the macromolecule, have negative values. Moreover, the virial coefficients of the c^n terms should also usually be negative. Experimental results show the virtual elimination of such charge-fluctuation effects in the presence of a moderate amount of salt. Since virial effects are found for other solution parameters, such as sedimentation coefficients, intrinsic viscosities, and linear as well as rotational diffusion coefficients, charge fluctuations can be expected to affect these hydrodynamic parameters also.

¹ C. Tanford, "Physical Chemistry of Macromolecules," pp. 227, 293, 352, 563. Wiley, New York, 1961.

² H. K. Schachman, "Ultracentrifugation in Biochemistry," pp. 226ff. Academic Press, New York, 1959.

³ K. O. Pedersen, in "The Ultracentrifuge" (T. Svedberg and K. O. Pedersen, eds.), p. 16. Oxford Univ. Press (Clarendon), London and New York, 1940.

⁴ A. Tiselius, *Kolloid-Z.* **59**, 306 (1932).

⁵ F. Booth, *J. Chem. Phys.* **22**, 1956 (1954).

⁶ K. O. Pedersen, *J. Phys. Chem.* **62**, 1282 (1958).

⁷ S. N. Timasheff and M. J. Kronman, *Arch. Biochem. Biophys.* **83**, 60 (1959).

¹⁰ M. J. Kronman and S. N. Timasheff, *J. Phys. Chem.* **63**, 629 (1959).

¹¹ S. N. Timasheff, in "Electromagnetic Scattering-I.C.E.S." (M. Kerker, ed.), p. 33. Macmillan, New York, 1963.

¹² J. G. Kirkwood and J. B. Shumaker, *Proc. Natl. Acad. Sci. U.S.A.* **38**, 863 (1952).

¹³ J. G. Kirkwood and S. N. Timasheff, *Arch. Biochem. Biophys.* **65**, 50 (1956).

¹⁴ S. N. Timasheff, H. M. Dintzis, J. G. Kirkwood, and B. D. Coleman, *J. Am. Chem. Soc.* **79**, 782 (1957).

¹⁵ S. N. Timasheff and I. Tinoco, *Arch. Biochem. Biophys.* **66**, 427 (1957).

¹⁶ S. N. Timasheff and B. D. Coleman, *Arch. Biochem. Biophys.* **87**, 63 (1960).

Specifically, the translational diffusion coefficient D_t and the rotary diffusion coefficient D_r exhibit the influence of the activity coefficient, γ , which expresses the combined result of all such effects, according to

$$D_t = (8/6)D_r = [kT/(6\pi\eta r_s)](1 + cd \ln \gamma/dc) \quad (3)$$

where k is Boltzmann's constant, 1.3806×10^{-16} erg $^\circ\text{K}^{-1}$, T is the temperature in K, η is the viscosity of the solvent, and r_s is the Stokes radius of the macromolecule. Accordingly, electrostatic repulsion and charge fluctuation will affect these, as well as other hydrodynamic parameters.

Measurements of protein hydration by NMR relaxation techniques using the two-state model of Zimmerman and Brittin¹⁷ have yielded surprisingly large values for the correlation time τ_c of bound water when cross-relaxation effects were avoided by experiments in D_2O .^{18,19} When cross-relaxation effects were not taken into account (e.g., in proton NMR of water), correlation times obtained from dispersion data also were high,¹⁸⁻²¹ even though Andree²² had shown that apparent τ_c values from frequency dependence of spin-lattice relaxation should be smaller as a result of cross relaxation. Also, recent ^{17}O NMR T_1 and T_2 data of Halle *et al.*²³ give τ_c values larger than would be predicted by the Debye-Stokes-Einstein equation, a result attributed by the authors to long-range coulombic protein-protein interactions. However, these measurements as well as many others were made, again, on isoionic protein solutions with no added salt. But since rotary diffusion is basic to these measurements (i.e., the bound water rotates with substantially the same τ_c as the protein) and is related to τ_c by $\tau_c = r_s^2/6D_r$, it can be seen from Eq. (3) that

$$\tau_c = [4\pi\eta r_s^3/(3kT)](1 + cd \ln \gamma/dc)^{-1} \quad (4)$$

and consequently, not only electrostatic effects due to the high charge-to-mass ratio of the protein but also charge-fluctuation effects should be encountered, both as a result of the methodology of these measurements. The absence of salt and the consequently large negative virial coefficients thus account for the excessive apparent τ_c values observed. The addition of salt should then result in correlation times more in accord with those

¹⁷ J. R. Zimmerman and W. E. Brittin, *J. Phys. Chem.* 1328 (1957).

¹⁸ K. Hallenga and S. H. Koenig, *Biochemistry* 15, 4255 (1976).

¹⁹ S. H. Koenig, K. Hallenga, and M. Shporer, *Proc. Natl. Acad. Sci. U.S.A.* 72, 2667 (1975).

²⁰ S. H. Koenig and W. E. Schillinger, *J. Biol. Chem.* 244, 3283 (1968).

²¹ T. R. Lindstrom and S. H. Koenig, *J. Magn. Reson.* 15, 344 (1974).

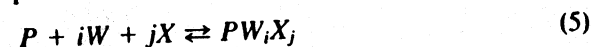
²² P. J. Andree, *J. Magn. Reson.* 29, 419 (1978).

²³ B. Halle, T. Andersson, S. Forsén, and B. Lindman, *J. Am. Chem. Soc.* 103, 500 (1981).

calculated for the protein directly from structural considerations. In fact, two recent studies,^{24,25} using different means to deal with the complicating effects of cross relaxation but both using salt, obtained τ_c values in good agreement with the known structure.

Since, to address this problem, one clearly should work with solutions containing salt, the theory now needs to be expanded to accommodate a three-component system. Expressions for NMR relaxation rates are rederived here in terms of the multicomponent theory of Casassa and Eisenberg,²⁶ since now the salt components can compete with water for binding sites on the protein molecule (e.g., charged side chains). The expressions embodying this theory are then tested against concentration-dependent spin-lattice and spin-spin relaxation data on β -lactoglobulin A (β -Lg A) in D_2O and H_2O under associated and unassociated conditions.²⁴

The model used as a point of departure for this derivation is a fast-exchange two-state, three-component system. The initial assumptions are (1) only one correlation time exists for the bound-water state, (2) there is competition between bound water and salt for the interaction sites on the surface of the protein, but (3) there is no competition between salt and protein for water since experiments will be performed only on protein solutions with added salt, not on insoluble or powdered samples. Hence, a general equilibrium expression for the binding is



where P , W , and X represent protein, water, and salt at free concentrations p , w , and x , bound concentrations p_b , w_b , and x_b , and total concentrations

$$P = p + p_b, \quad W = w + w_b, \quad \text{and} \quad X = x + x_b \quad (5a-c)$$

respectively. Associated with the formation of each species PW_iX_j is an apparent macroscopic association constant K_{ij} . Then

$$p_b = p \sum_{i=0}^q \sum_{j=0}^r K_{ij} w^i x^j \quad (6a)$$

where q and r are any positive integers such that $q + r = n$, the total number of binding sites per molecule. At the same time,

$$w_b = p \sum \sum i K_{ij} w^i x^j \quad \text{and} \quad x_b = p \sum \sum j K_{ij} w^i x^j \quad (6b,c)$$

²⁴ T. F. Kumosinski and H. Pessen, *Arch. Biochem. Biophys.* 218, 286 (1982).

²⁵ H. Pessen, J. M. Purcell, and H. M. Farrell, Jr., *Biochim. Biophys. Acta* 828, 1 (1985).

²⁶ E. F. Casassa and H. Eisenberg, *Adv. Protein Chem.* 19, 287 (1964).

The average number of molecules of water or salt bound to a molecule of protein, i.e., the Scatchard hydration, $\bar{\nu}_w$, and salt binding $\bar{\nu}_x$, respectively, are then given by

$$\bar{\nu}_w = w_b/P \quad \text{and} \quad \bar{\nu}_x = x_b/P \quad (6d,e)$$

which may be also written in terms of the Eqs. (6a-c). (We designate here as Scatchard hydration all protein-water interactions characterized by multiple equilibria. Another type of water binding, preferential hydration, will be encountered further on. For a particularly clear exposition of the relationships between these concepts, see Ref. 27.)

The concentrations are commonly expressed in moles/liter but may, when convenient, equally well be expressed in moles/1000 g water, as will be the case in the following. While this will change the numerical values and dimensions of association constants, $\bar{\nu}_w$ and $\bar{\nu}_x$ will remain unaffected. Strictly speaking, all terms should be expressed as the corresponding activities rather than as molar or molal concentrations. (However, in view of the generally large molecular weights of proteins, even fairly concentrated solutions are usually no more than $10^{-13} M$ and, under the conditions of many experiments, virial coefficients are negligible; i.e., the protein has a small net charge. Deviations from this last assumption will be discussed specifically later.)

The experimentally derived quantity to be considered is the slope of the plot of either the spin-lattice (R_1) or the spin-spin (R_2) relaxation rate of the water vs the concentration of protein present. In analogy to other quantities encountered in solution theory, the slope $(dR/dP)_\mu$ may be termed the relaxation increment; the subscript μ indicates that solutions are at constant chemical potential and, in terms of experimental procedure, that exhaustive dialysis against buffer was performed prior to the proton NMR relaxation measurements.

Considering now the relaxation increment of an aqueous solution of protein in the presence of salt as a concentration-dependent function, and expressing the total relaxation rate of the water in the three-component system in terms of the solution components, one may write, on the basis of fast exchange of water between two fractions of rates R_b (for bound water) and R_f (for free water), and in view of Eq. (6b),

$$R = \frac{w_b}{W} R_b + \frac{w}{W} R_f = \frac{(p \sum \sum i K_{ij} w^i x^j) R_b + w R_f}{p \sum \sum i K_{ij} w^i x^j + w} \quad (7)$$

From R as a function of P , W , and X , one has the total derivative

$$\left(\frac{dR}{dP}\right)_\mu = \left(\frac{\partial R}{\partial P}\right)_{w,x} + \left(\frac{\partial R}{\partial W}\right)_{p,x} \left(\frac{dW}{dP}\right)_\mu + \left(\frac{\partial R}{\partial X}\right)_{p,w} \left(\frac{dX}{dP}\right)_\mu \quad (8)$$

The coefficients of the three terms can be evaluated by partial differentiation of Eq. (7) with the use of Eqs. (6a-c). More directly, from Eqs. (7) and (5b) (where w , because of the exhaustive dialysis, is a constant),

$$R = \frac{(W - w)R_b + wR_f}{W} = R_b - (R_b - R_f) \frac{w}{W} \quad (9)$$

and from this,

$$\left(\frac{\partial R}{\partial P}\right)_{w,x} = 0, \quad \left(\frac{\partial R}{\partial W}\right)_{p,x} = \frac{(R_b - R_f)w}{W^2}, \quad \left(\frac{\partial R}{\partial X}\right)_{p,w} = 0 \quad (9a)$$

and therefore

$$\left(\frac{dR}{dP}\right)_\mu = \left(\frac{\partial R}{\partial W}\right)_{p,x} \left(\frac{dW}{dP}\right)_\mu = \frac{(R_b - R_f)w}{W^2} \left(\frac{dW}{dP}\right)_\mu \quad (10)$$

From Eqs. (5b) and (6d), $W = w + w_b = w + \bar{\nu}_w P$ and, with $dw/dP = 0$,

$$\left(\frac{dW}{dP}\right)_\mu = \bar{\nu}_w \quad (11)$$

Because $w_b \ll W$, $w \approx W$ (≈ 55.6), and Eq. (10) becomes

$$\left(\frac{dR}{dP}\right)_\mu = \frac{R_b - R_f}{W} \bar{\nu}_w \quad (12)$$

Since protein molecular weights are not always precisely known, it is convenient to replace the molality P by the concentration c (in g protein/g water) and the hydration $\bar{\nu}_w$ (in moles/mole) by $\bar{\nu}'_w$ (in the conventional units of g bound water/g protein). Then $c = PM_p/1000$ and $\bar{\nu}'_w = \bar{\nu}_w M_w/M_p$, where M_p and M_w are the molecular weights of protein and water, respectively. Also, $dP/dc = 1000/M_p$ and $(1000/W)M_w$ being unity),

$$\left(\frac{dR}{dc}\right)_\mu = \left(\frac{dR}{dP}\right)_\mu \left(\frac{dP}{dc}\right) = (R_b - R_f) \bar{\nu}'_w \quad (13)$$

In the present work the relationship of R to c (as shown in Fig. 1 for both R_1 and R_2 results) was linear. One may write Eq. (9) alternatively as

$$R = R_f + (R_b - R_f) \frac{w_b}{W} = R_f + (R_b - R_f) \frac{P\bar{v}_W}{W}$$

$$= R_f + (R_b - R_f)c\bar{v}'_W \quad (13a)$$

and from Eqs. (13) or (13a), with a constant relaxation increment,

$$(dR/dc)_\mu = (R_b - R_f)\bar{v}'_W = k \quad (13b)$$

or

$$R = R_f + (R_b - R_f)c\bar{v}'_W = R_f + kc \quad (13c)$$

Absence of such linearity might be due to polydispersity and consequent changes in the $(R_b - R_f)$ factor, which would have to be allowed for. The other factor in the relaxation increment, \bar{v}_W , is generally taken to be independent of protein concentration (cf. Ref. 28). If it is not actually constant, an additional term accounting for its concentration dependence would have to be included in Eqs. (13b,c), unless a change from concentration units to activities will remove the nonlinearity, as discussed under Analysis of Data.

If it is desired to express protein concentrations as c_2 in g protein/ml solution, the solution density ρ and the concentration of the third component, c_3 , need to be known, whereupon

$$c = \frac{c_2}{\rho - c_2 - c_3} \quad (14)$$

and

$$\left(\frac{dR}{dc_2}\right)_\mu = k \frac{\rho - c_3}{(\rho - c_2 - c_3)^2} \quad (14a)$$

The need to know solution densities may be eliminated for all except very high protein concentrations with a knowledge of the partial specific volume \bar{v} and the solvent density ρ_0 . From the definition of \bar{v} it can then be shown that

$$c = \frac{c_2}{\rho_0(1 - \bar{v}c_2) - c_3} \quad (14')$$

and

$$\frac{dR}{dc_2} = k \frac{\rho_0 - c_3}{[\rho_0(1 - \bar{v}c_2) - c_3]^2} \quad (14'a)$$

In cases of high protein concentration the more general Eqs. (14), (14a) may have to be used. At low protein concentration, where $\rho_0 \approx 1.0$ while

$c_2, c_3 \ll \rho$, Eqs. (14a) and (14'a) reduce to expressions formally identical to Eq. (13b) with c_2 in place of c ; a corresponding remark is true for Eqs. (14) and (14') with respect to Eq. (13c).

From Eq. (13b), $R_b = (k/\bar{v}'_W) + R_f$ for either R_1 or R_2 , and therefore

$$R_{2b}/R_{1b} = (k_2 + R_{2f}\bar{v}'_W)/(k_1 + R_{1f}\bar{v}'_W) \quad (15)$$

But generally $R_f\bar{v}'_W \ll R_b$, hence, from the definition of k , one obtains the useful approximation

$$R_{2b}/R_{1b} \approx k_2/k_1 \quad (15a)$$

The parameters k_1 , R_{1f} , k_2 , and R_{2f} are experimentally accessible as the slope k and intercept R_f from R_1 or R_2 vs c_2 plots, respectively, such as those of Fig. 1.

Use of these relationships in conjunction with the Kubo-Tomita-Solomon equations,^{29,30} which relate R_{1b} and R_{2b} to the correlation time of the bound water, will give the requisite number of equations to permit simultaneous solution for \bar{v}'_W and τ_c . These equations may be written as

$$R_{1b} = 2K\tau_c[(1 + \omega_0^2\tau_c^2)^{-1} + 4(1 + 4\omega_0^2\tau_c^2)^{-1}] \quad (16a)$$

and

$$R_{2b} = K\tau_c[3 + 5(1 + \omega_0^2\tau_c^2)^{-1} + 2(1 + 4\omega_0^2\tau_c^2)^{-1}] \quad (16b)$$

where $\omega_0 = 2\pi\nu_0$ is the nuclear angular precession frequency for the nuclide observed, in radians/sec, and K is a measure of the strength of the nuclear interaction, viz.

$$K_{\text{deuterons}} = (3/80)(e^2qQ/\hbar)^2(\beta\eta/\beta + 1)S_{\text{deut}}^2 \quad (16c)$$

and

$$K_{\text{protons}} = (3/20)\hbar^2\gamma^4r^{-6}S_{\text{prot}}^2 \quad (16d)$$

Here e is the electronic charge, 1.6022×10^{-19} C, q is the electric field gradient, Q is the nuclear electric quadrupole moment, \hbar is Planck's constant divided by 2π , 1.0546×10^{-27} erg·sec; η is a dimensionless parameter measuring the deviation from axial symmetry³¹; γ is the gyromagnetic ratio for the proton, 2.6752×10^4 rad·G⁻¹·sec⁻¹; r is the internuclear proton distance for water, 1.526 Å; and S_{deut} and S_{prot} are respective order parameters.²³ It may be noted that these expressions assume no particular model for the relaxation mechanism accompanying NMR hydration. The

²⁹ R. Kubo and K. Tomita, *J. Phys. Soc. Jpn.* 9, 888 (1954).

³⁰ I. Solomon, *Phys. Rev.* 99, 559 (1955).

³¹ A. Abragam, "The Principles of Nuclear Magnetism," Chapter 8. Oxford Univ. Press, London and New York, 1961.

thermodynamic theory can be used whether isotropic relaxation ($S = 1$) or anisotropy of the bound water ($S < 1$) is hypothesized, where in the latter case the "bound" should be understood in the sense of "hydrodynamically influenced layers" or "surface-induced probability distribution of water molecules."^{23,32,33} The above treatment can easily be extended to a model postulating three or more states.

Experimental Procedures. Preparation of solutions. The following procedures are described to illustrate methods that have led to satisfactory results in a study of the whey protein β -lactoglobulin (β -Lg) in solution.²⁴ Protein solutions to be used for proton resonance measurements, prepared 1 day before use, were exhaustively dialyzed overnight against buffer at 0–5°; dilutions for the concentration series to be studied were made with the appropriate dialyzate. Solutions to be used for deuteron resonance measurements were made up from a stock solution prepared by partial deuterium exchange. A suitable amount of crystalline protein in a stoppered vial was allowed to equilibrate repeatedly for 24-hr periods at 4° as a slurry with a small quantity of D₂O, followed by high-speed centrifugation and addition of fresh D₂O, for a total of five times. The solutions were buffered by direct addition of solid potassium phosphate, and the pH was adjusted by addition of 0.1 N NaOD in D₂O. Concentrations of β -Lg were determined spectrophotometrically from an absorption coefficient of 0.96 ml mg⁻¹ cm⁻¹ at 278 nm.³⁴

Relaxation measurements. Resonance relaxation spectra were obtained by Pulse Fourier Transform spectroscopy with a JEOL FX60Q spectrometer³⁵ operating at a nominal frequency of 60 MHz. The frequency of observation for protons was 59.75 MHz; for deuterons, 9.17 MHz. Raw data were in the form of relative intensities as calculated by the JEOL 980B computer.

Since the high concentration of water in a dilute solution produces an intense signal, a single accumulation at the particular sample temperature (2, 10, or 30 ± 1°) was sufficient for each spectrum. Even then, care was necessary to avoid exceeding the dynamic range of the computer with consequent truncation. To this end, as well as to economize on the limited amount of the A variant of the protein available, small sample volumes were employed by use of a microcell assembly with an expendable 35- μ l sample bulb, available from Wilmad Glass Company, Inc. The protein

solution was introduced very slowly into the spherical bulb by means of a fine-gauge syringe needle inserted through its capillary neck, to avoid the inclusion of any air bubbles which, if trapped below the neck, could lead to vortex formation in the spinning sample bulb and vitiate the necessary assumption of spherical sample geometry. The bulb, suspended by its neck from a chuck attached to a plastic cap, was positioned snugly inside a precision 5-mm-o.d. sample tube which, initially, contained also the lock-signal solvent. The small amount of this solvent in the residual annular space outside the bulb was not always sufficient to assure maintenance of the lock; occasional failure of the lock during a lengthy series of automatic measurements resulted in loss of usable data. A second arrangement was then used in which the 5-mm tube, containing the sample bulb but no solvent, was positioned by means of fluorocarbon plastic spacers concentrically within a precision 10-mm-o.d. sample tube accommodating a much larger quantity of lock-signal solvent. Incidental advantages of this arrangement were that the outside of the sample bulb was thus kept dry, and that the solvent could be sealed within the annular space between the two tubes and so kept from contamination for a greatly extended time. Except for these advantages, either arrangement resulted in the same measurements. The cell assembly, in either case, was positioned in the JEOL FX60Q 10-mm ¹H/¹³C dual probe insert.

Longitudinal (spin-lattice) relaxation rates R_1 were measured by the inversion-recovery method,³⁶ where the repetition time T in the pulse sequence [... T ... π ... τ ... $\pi/2$...] was chosen to be at least five times T_1 ($\equiv R_1^{-1}$) and the values of the variable delay time τ ranged from 10 msec to 3 sec, for a total of between 5 and 20 τ -values, depending on the detail desired. From the Bloch equations³⁷ under the conditions of this method, the relation of the peak intensity A_τ to the pulse delay time τ becomes

$$A_\tau = A_\infty [1 - 2 \exp(-R_1 \tau)] \quad (17)$$

where A_∞ is the limiting peak intensity for $\tau \rightarrow \infty$. Independent measurement of A_∞ , a source of irreducible error, can be dispensed with, and the problem of weighting the data points in the conventional linear plot (logarithm of a function of relative peak heights vs τ) can be eliminated, by fitting directly to the data points (τ, A_τ) by least-squares an exponential of the form of Eq. (17), from which the two parameters A_∞ and R_1 can be obtained.

The factor 2 preceding the exponential in Eq. (17) is based on theory which predicts $A_\infty = -A_0$, where A_0 is the peak intensity for $\tau = 0$. It is

recognized that in point of fact this equality rarely holds exactly because of slightly imperfect adjustment of the flip angle π . When Eq. (17) is used in its logarithmic form, A_∞ must be determined by explicit measurement, and A_0 then is usually seen, from the ordinate intercept of the straight-line plot of $\ln(A_\infty - A_\tau)$ vs τ , to differ somewhat from its theoretical value. This, however, is essentially without relevance with respect to the only parameter of intrinsic interest, namely the R_1 obtained from the slope, except possibly insofar as agreement of the intercept with $\ln 2A_\infty$ would be some measure of the quality of the data as a whole. When the equation is used, as it is here, in the exponential form with A_∞ not explicitly determined, the assumption $A_\infty = -A_0$ implies a two-parameter exponential fit, whereas $A_\infty \neq -A_0$ would imply a three-parameter exponential fit. The latter has been advocated or practiced in the past by various authors.³⁸⁻⁴¹ Such a practice, however, has ignored the definitive treatment of this matter by Leipert and Marquardt,⁴² concurred in by Becker *et al.*,⁴³ which has shown conclusively that introduction of a third adjustable parameter, so far from improving the statistics, leads to a significant loss of precision in the estimate of R_1 because of an undesirable correlation between what should be statistically independent parameters, R_1 and A_∞ . The effect, on the other hand, of even a considerably misadjusted flip angle on the value of R_1 obtained was shown to be insignificant for values of $R_1 > 0.1$ sec, a condition generally satisfied.

The fitting of the two-parameter exponential was carried out by computer by means of an iterative program. For each sample R_1 was determined at least four times, and the results were averaged. This procedure was repeated at each concentration; a minimum of six concentrations were used under each set of conditions of temperature and pH at which the resonance relaxation of each nuclide was examined.

Transverse (spin-spin) relaxation rates R_2 were determined by spin-locking measurement⁴⁴ of $R_{1\rho}$, the longitudinal relaxation rate in the rotating frame. $R_{1\rho}$ equals R_2 in dilute solutions of low viscosity whenever the magnitude of $R_{1\rho}$ is independent of $H_{1\rho}$, the spin-locking radio-frequency field in the rotating frame; this was the case, within the limits of experi-

mental error, in the present work. R_2 was evaluated as described above for R_1 , except that the relation between peak intensity A_τ and decay time τ derived from the Bloch equations in this case becomes

$$A_\tau = A_0 \exp(-R_2\tau) \quad (18)$$

where the initial intensity A_0 replaces A_∞ as the maximum peak intensity. Again, a least-squares two-parameter exponential fit to the data points was performed by an iterative computer program, from which A_0 and R_2 were obtained.

For each sample, R_2 was determined with the same number of replications as R_1 . Measurements of one mode of relaxation were made on the identical samples and immediately following the completion of measurements of the other mode, or at latest the next day. In this manner, measurements for proton relaxation at 59.75 MHz were made at pH 6.2 at 2 and 30°, at pH 4.65 at 2 and 30°, and at pH 2.7 at 10°. Measurements for deuteron relaxation at 9.17 MHz were made at pH 6.2 and 4.65, at both 2 and 30°.

Analysis of Data. Activities and the multicomponent expression. An observation regarding predictions resulting from the derived multicomponent expressions may immediately be in order. Since these are based ultimately on equilibrium constants, the mass terms should be properly expressed as activities instead of concentrations. Consequently, relaxation rate vs concentration curves should be expected to be nonlinear whenever there are appreciable protein activity coefficients. Figure 1 shows concentration dependences of R_1 and R_2 for β -Lg A at pH 6.2 and 30°, and of R_2 at pH 4.65 and 2°. Under these conditions the charge-to-mass ratio and the second virial coefficient are relatively small ($B_0 = 0.9$ ml/g).³⁴ In fact, all these data exhibit linear relationships over a concentration range from 0 to 0.08 g protein/g water, where γ does not differ greatly from unity. Figure 2, on the other hand, shows corresponding plots for pH 2.7 and 10°, where the net charge is approximately 40 and the second virial coefficient is 8.5 ml/g.⁴⁵ The plots in terms of concentration here are clearly nonlinear. A change in the concentration scale to g protein/g water had no significant effect on the nonlinearity of the plots. (Low-temperature data were used at this pH for experimental reasons: the protein under these conditions undergoes a dissociation from dimer to monomer, but the amount of monomer at low temperature at concentrations in excess of 0.01 g/ml is negligible.⁴⁵)

A polynomial curve-fitting program was used with all data on Figs. 1 and 2 as well as all other concentration-dependent data in order to deter-

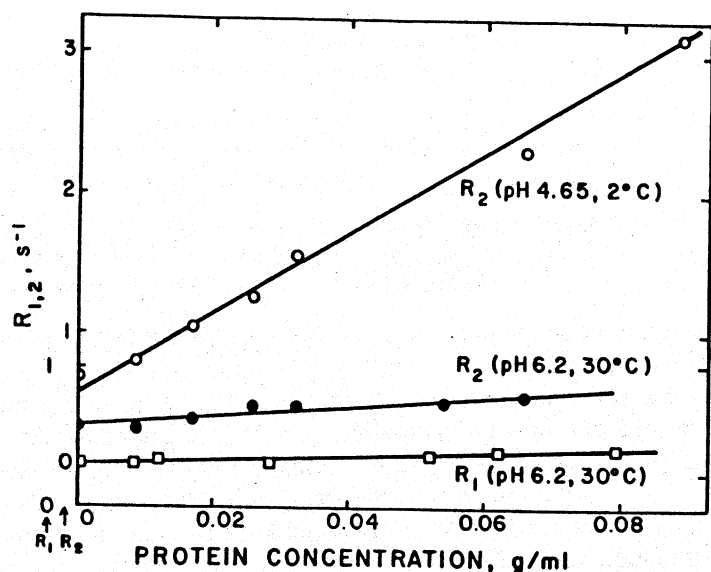


FIG. 1. Dependence of proton relaxation rates on β -lactoglobulin A concentrations (g protein/g water) in H_2O . Transverse relaxation rates R_2 at pH 4.65 and 2° (\circ) and at pH 6.2 and 30° (\bullet). Longitudinal relaxation rates R_1 (\square) at pH 6.2 and 30° (shown for comparison only; not used in calculations). Points represent experimental values; lines represent least-squares fits. All points show linear relationship of relaxation rates to concentration at pH 4.65 and 6.2. (Taken from Ref. 24.)

mine linearity or nonlinearity, the degree of the polynomial being determined by goodness of fit as judged by F test. (The regression program used selects the lowest degree expression for which the sum of squares due to the addition of one higher degree is statistically insignificant.) The two concentration plots of Fig. 2 give polynomials of degree two. Protein concentrations, c , were then transformed into activities, a , by means of the relationship $a = \gamma c$, where the activity coefficient $\gamma = \exp(2B_0c)$ was obtained [see Eq. (2)] from the second virial coefficient $B_0 = 8.5$ ml/g, as cited above. Activity plots corresponding to the concentration plots are also shown in Fig. 2; it is evident that these are linear by the same criteria.

Under the conditions of Fig. 2, γ is sensibly larger than unity and, even in the presence of salt, failure to treat R as a function of activity rather than concentration will evidently lead to excessively high values of hydration [cf. Eq. (13c)]. The opposite would be true under conditions when, in the absence of salt, charge fluctuations and consequent intermolecular attraction exist. With γ less than unity, a concentration plot in place of the correct activity plot for R must lead to inordinately low values

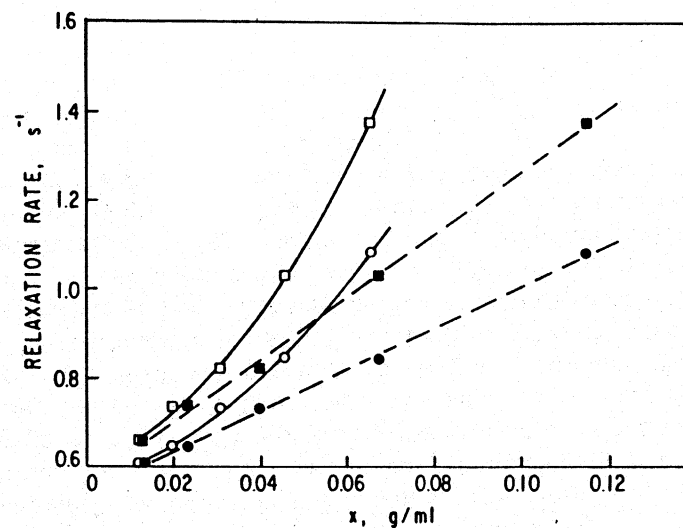


FIG. 2. Dependence of water proton relaxation rates of β -lactoglobulin A on both concentration and activity, at pH 2.7 and 10° . Transverse relaxation rates (squares) as function of X (\square , X = concentration; \blacksquare , X = activity). Longitudinal relaxation rates (circles) as function of X (\circ , X = concentration; \bullet , X = activity). All points represent experimental values; lines represent least-squares polynomial fits of highest degree to make a statistically significant contribution to goodness of fit (F test). Dependence on concentration is found to be of second degree as consequence of charge effects at pH 2.7. (Polynomial coefficients for R_1 , $a_0 = 0.562$, $a_1 = 2.926$, $a_2 = 75.86$; for R_2 , $a_0 = 0.606$, $a_1 = 3.468$, $a_2 = 125.9$.) Activities take these effects into account, and dependence on activities is linear. (Coefficients of straight line: for R_1 , $a_0 = 0.541$, $a_1 = 4.691$; for R_2 , $a_0 = 0.560$, $a_1 = 7.061$.) (Taken from Ref. 24.)

of hydration. Alternatively, protein concentrations could continue to be used, provided the right-hand side of Eq. (13) is multiplied by $(da/dc)_\mu$.

These results may be taken to demonstrate the validity of the multi-component expression. This expression will be used in the following in analyzing the data to describe the hydration of the genetic A variant of β -lactoglobulin, β -Lg A, under nonaggregation conditions, as well as under the well-characterized dimer-to-octamer association.⁴⁶⁻⁵⁰ (This phenomenon, because it involves a 4-fold association of dimer under conditions where dissociation to monomer is negligible, will be referred to in the following as "tetramerization.") It has been demonstrated that here the

⁴⁶ J. Witz, S. N. Timasheff, and V. Luzzati, *J. Am. Chem. Soc.* **86**, 168 (1964).

⁴⁷ R. Townend and S. N. Timasheff, *J. Am. Chem. Soc.* **82**, 3168 (1960).

⁴⁸ T. F. Kumosinski and S. N. Timasheff, *J. Am. Chem. Soc.* **88**, 5635 (1966).

⁴⁹ S. N. Timasheff and R. Townend, *J. Am. Chem. Soc.* **83**, 464 (1961).

⁵⁰ S. N. Timasheff and R. Townend, *Protides Biol. Fluids* **16**, 33 (1969).

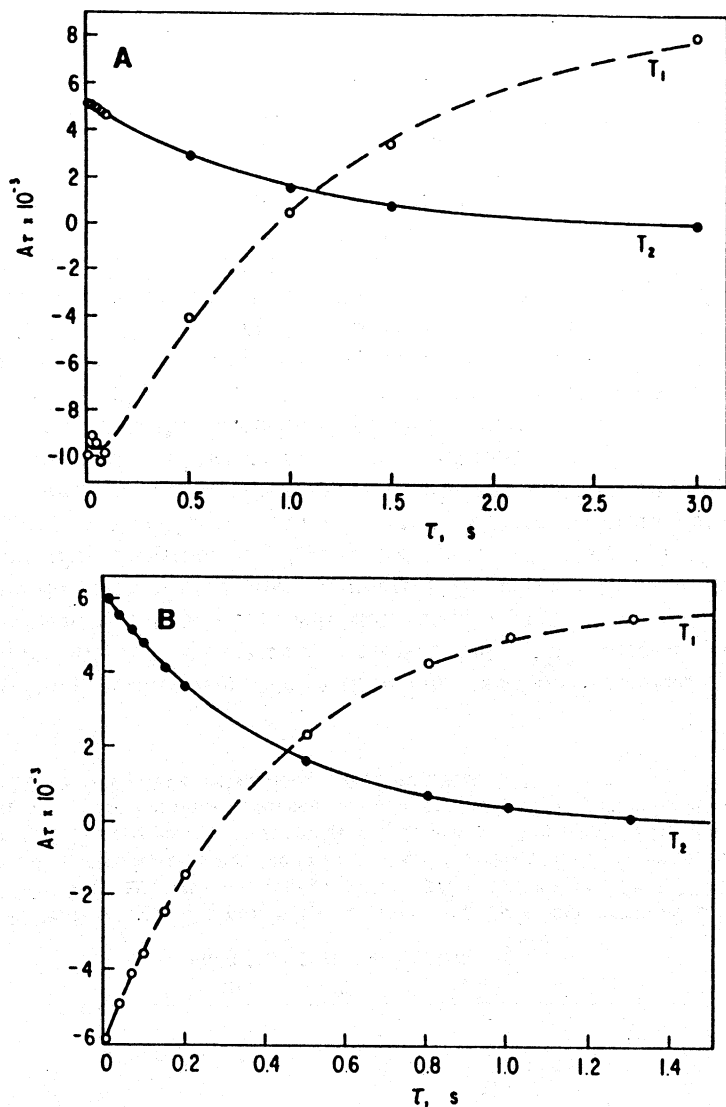


FIG. 3. (A) Proton resonance peak intensities A as functions of time τ , for solutions of β -Lg A in H_2O (6.09×10^{-2} g protein/g H_2O) at pH 6.2, 30° . Intensities for transverse relaxation (T_2 , \bullet) as function of decay time, from spin-locking measurements of $T_{1\rho}$; intensities for longitudinal relaxation (T_1 , \circ) as function of delay time, from inversion-recovery measurements. Points represent experimental values. Line for T_2 represents two-parameter exponential fit. Line for T_1 represents four-parameter double-exponential fit; need for this fit shown by initial course of this line, indicative of cross-relaxation. (B) Deuteron resonance peak intensities A as function of time τ , for solutions of β -Lg A in D_2O (2.86×10^{-2} g protein/g D_2O) at pH 6.2, 30° . In this case, the indication of cross-relaxation in T_1 is absent and a two-parameter exponential shows excellent fit to the experimental points even at shortest times. (A and B, taken from Ref. 24).

virial coefficients are small,^{34,45} so that it is permissible to simplify the treatment by using protein concentrations.

Isotropic binding, two-state model. Determination of correlation times. Proton spin-spin relaxation measurements of water in solutions of β -Lg A gave results indicating a single relaxation rate, whereas spin-lattice results could be fitted only by the sum of two exponential functions (Fig. 3A). This behavior is consistent with the work of Edzes and Samulski⁵¹ and others,^{22,52} who found a cross-relaxation mechanism between the water-bound protons and the protein protons to make a significant contribution to the spin-lattice relaxation rate in water-collagen systems. Subsequently, Koenig *et al.*⁵³ showed that cross-relaxation also exists in spin-lattice relaxation (T_1 processes) in globular protein solutions, i.e., the cross-relaxation rate disperses as a T_1 process and not as a T_2 process. With the notation of Edzes and Samulski, for the solution illustrated in Fig. 3A parameters in the equation $m(t) = c^+ \exp(-R_1^+ t) + c^- \exp(-R_1^- t)$ are $R_1^+ = 15.0$, $R_1^- = 0.45$, $c^+ = 0.01$, and $c^- = 1.01$, where the reduced magnetization $m(t) \equiv (A_x - A_z)/2A_x$. The statistics here were poor because of instrument limitations.⁵⁴ (Cross relaxation, calculated for β -Lg in a novel way,²⁵ was found to contribute to the observed apparent spin-lattice relaxation to the extent of about 90%.) As an alternative approach, protein solutions were made up in D_2O , and the dependence of R_1 and R_2 on protein concentration was measured by deuteron NMR at 9.17 MHz which, in effect, eliminated cross relaxation from the T_1 measurements (Fig. 3B). The concentration dependence of R_2 of protons in solutions of β -Lg A in H_2O under the same environmental conditions was also measured (Fig. 1).

Concentration plots of R_1 and R_2 for D_2O (Fig. 4) showed no evidence of nonlinearity, at either pH and either temperature, over the concentration range studied. This agrees with the low virial coefficient of β -Lg A under these conditions.³⁴ The relaxation increments k_1 and k_2 , together with the corresponding intercepts R_{1f} and R_{2f} (Fig. 4), were used in Eqs. (13) and (16) to determine the bound-water correlation times τ_c presented in Table I. As can be seen, τ_c increased as the temperature decreased; this is in quantitative agreement with the requirement of Stokes' equation that τ_c increase with both increasing viscosity and decreasing temperature. Furthermore, τ_c also increased when the pH was lowered from 6.2 to 4.65,

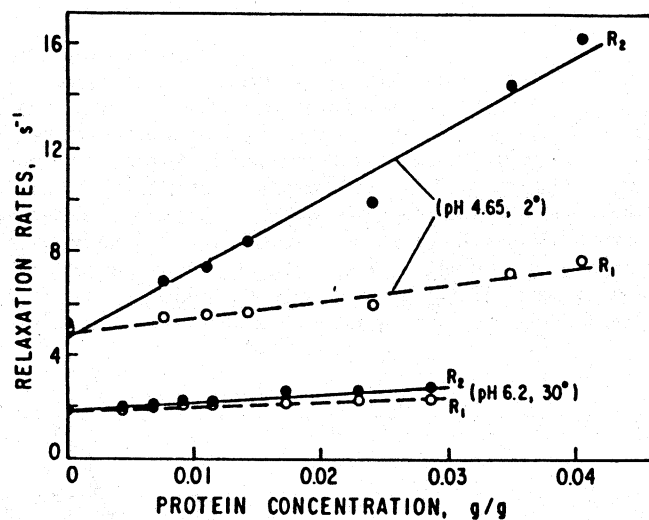


FIG. 4. Dependence of deuteron relaxation rates on β -Lg A concentrations (g protein/g water) in D_2O . Transverse relaxation rates R_2 (●) at pH 4.65, 2° and at pH 6.2, 30°. Longitudinal relaxation rates R_1 (○) under the same two sets of conditions. Points represent experimental values; lines represent least-square fits. Points at all concentrations show linear relationship of relaxation rates to concentration, at both sets of pH and temperature conditions, and for both modes of relaxation. (Taken from Ref. 24.)

as would be predicted from the work of Timasheff and Townend,⁵⁵ which showed that β -Lg A associates at the lower, but not at the higher pH, and that the association increases with decreasing temperature.

Determination of hydration parameters. Since the extent of a possible intermolecular contribution, R_{2b}^i , to the spin-spin relaxation of bound-water protons and the number of protein protons so contributing are unknown, determination of Scatchard hydrations was attempted by three different methods and the results were compared.

Method I. Only the deuterium NMR relaxation increments were used, with a value of $e^2qQ/\hbar = 215.6$ kHz⁵⁶ and with the asymmetry parameter η assumed to be zero. This type of calculation gives low values of $\bar{\nu}'_w$, as shown in Table II; however, low values could be expected because the relaxation increment probably samples only a percentage of the total hydration of a protein, since at 9.17 MHz any bound water with τ_c values less than 6 nsec would have a T_1/T_2 ratio of unity. At pH 4.65, where tetramerization occurs, the hydration markedly increases with decreasing

TABLE I
DEUTERON NMR RELAXATION AND HYDRODYNAMIC RESULTS FOR β -LACTOGLOBULIN IN SOLUTION^a

pH	T, °C	k_1^b	k_2	R_{1r} , sec ⁻¹	R_{2r} , sec ⁻¹	τ_c , nsec	r_{NMR}^c , Å	r_{sed}^c , Å	$(\tau_c)_{calc}$, nsec
6.2	30	20.7	31.9	1.93	1.93	10.0	23.2	27.0	10.2
		±0.9	±1.9	±0.01	±0.04	±2.7	±1.9		
4.65	30	17.9	58.9	5.46	5.25	25.6	30.4	43.5	22.5
		±2.1	±5.2	±0.24	±0.28	±4.1	±1.5		
4.65	30	25.4	73.2	2.01	1.79	22.5	30.4	43.5	65.9
		±1.9	±5.0	±0.04	±0.12	±3.3	±1.5		
4.65	2	63.9	274.2	4.90	4.67	32.2	30.4	43.5	145.0
		±7.1	±19.0	±0.16	±0.44	±4.6			

^a Adapted from Ref. 24.

^b Error terms in this and subsequent tables represent the standard error of the parameter.

^c Spherical model assumption.

TABLE II
HYDRATION AND THERMODYNAMICS FOR β -LACTOGLOBULIN FROM DEUTERON NMR
USING $(e^2qQ/h) = 215.6 \text{ kHz}^{a,b}$

pH	T, °C	$\bar{\nu}'_w$, g H ₂ O/g protein	ΔG , kcal	$-\Delta H$, kcal	$-\Delta S$, eu
6.2	30	0.0063 ± 0.0008	0.90 ± 0.08	0.8 ± 3.0	6 ± 10
	2	0.0072 ± 0.0020	0.74 ± 0.15		
4.65	30	0.0095 ± 0.0002	0.65 ± 0.01	6.9 ± 1.6	24.8 ± 5.8
	2	0.0301 ± 0.0003	-0.044 ± 0.006		

^a Adapted from Ref. 24.

^b Method I, as described under Analysis of Data.

temperature, whereas at pH 6.2, where none occurs, the hydration is lower and independent of temperature. This is consistent with the findings of Timasheff and co-workers^{46,57} from small-angle X-ray scattering that the geometry of the octamer must include a large central cavity in which trapped water could reside.

Method II. A combination of the τ_c values found by deuteron NMR at 9.17 MHz (Table I) and the k_2 values found from proton NMR at 59.75 MHz was used (Fig. 1). The reason for this procedure is that the quadrupole coupling constant for the bound water should actually decrease as hydrogen bonding increases.⁵⁸ Here R_{2b} can be calculated from Eq. (16b) at 59.75 MHz, and the $\bar{\nu}'_w$ values can be easily obtained from the simple relationship $\bar{\nu}'_w = k_2/(R_{2b} - R_{2f})$, derived from Eq. (13b). Such hydration values (Table III) are slightly higher than those from deuteron relaxation measurements only (Table II), but show the same temperature and pH dependence. (Combination experiments of this kind would be best performed at the same Larmor frequency; however, the availability of only a single spectrometer with no variable frequency capability would preclude this possibility. These experiments could shed light on such problems as the constancy of the hydrogen-bond distance under various conditions

TABLE III
HYDRATION AND THERMODYNAMICS FOR β -LACTOGLOBULIN DERIVED FROM τ_c VALUES OF TABLE I BY METHODS II AND III^a

pH	T, °C	k_2	R_{3r} , sec ⁻¹	$\bar{\nu}'_w$, g H ₂ O/g protein			ΔG , kcal	$-\Delta H$, kcal			$-\Delta S$, eu		
				II ^b	III ^c	III ^c		II ^b	III ^c	III ^c	II ^b	III ^c	III ^c
6.2	30	3.5 ± 0.5	0.34 ± 0.02	228	337	0.0152 ± 0.0021	0.103 ± 0.0007	0.35 ± 0.07	0.59 ± 0.04	0	0	1.2 ± 0.2	1.9 ± 0.1
				530	784	0.0152 ± 0.0008	0.0103 ± 0.0014	0.32 ± 0.03	0.54 ± 0.07				
4.65	30	9.2 ± 0.8	0.27 ± 0.04	468	694	0.0197 ± 0.0016	0.0133 ± 0.0011	0.20 ± 0.05	0.43 ± 0.04	4.62	4.62	15.9 ± 2.6	16.7 ± 2.4
				660	978	0.0428 ± 0.0017	0.0289 ± 0.0011	-0.25 ± 0.02	-0.032 ± 0.021	± 0.73	0.70		

^a Adapted from Ref. 24.

^b Method II uses τ_c from Table I and proton k_2 .

^c Method III uses, in addition to the procedure of Method II, the assumption $\bar{R}_{2b} = R_{2b} + 12 R_{2f}$, with the intermolecular proton distance for β -Lg A calculated from the partial specific volume as 2.61 Å, as described under Analysis of Data.

and the existence of a distribution of correlation times in the total hydration shell.)

Method III. This is a combination procedure also, with an extra intermolecular interaction term R'_{2b} added to the proton spin-spin relaxation rate R_{2b} . Based on the small-angle X-ray scattering results of Witz *et al.* for β -Lg A⁴⁶ in conjunction with the known molecular weight and amino acid composition, a simple consideration of the molecular geometry shows that, on the average, each proton in the protein will have six neighboring protons at a distance of 2.61 Å. From this average intermolecular distance, together with the τ_c values of Table I and the relationship $\bar{R}_{2b} = R_{2b} + 12 R'_{2b}$ (where \bar{R}_{2b} is the total spin-spin relaxation rate), the hydration can be calculated as $\bar{v}'_w = k_2/(\bar{R}_{2b} - R_{2b})$. These values (Table III) are in close agreement with those in Table I. Altogether, no great difference exists in the \bar{v}'_w values from all three methods.

Comparison of results with other structural information. Dynamics of β -Lg dimer. With the τ_c values calculated from k_2/k_1 from deuterium NMR spin-spin and spin-lattice relaxation increments, dR_2/dc and dR_1/dc , a Stokes radius r_{NMR} for the bound water can be calculated from the Stokes-Einstein relation⁵⁹ on the basis of a spherical model (Table I). At pH 6.2, where β -Lg A exists as the unassociated dimer, r_{NMR} is slightly lower than that for the protein itself derived from hydrodynamic data, r_{sed} .⁶⁰ This discrepancy could be due to the spherical approximation inherent in the use of the Stokes-Einstein equation, since the β -Lg dimer has an axial ratio of approximately 2:1.³⁴ Moreover, the Stokes radius of the protein obtained from sedimentation includes the water of hydration and should therefore be larger than the Stokes radius of the bound water calculated from the ²H NMR relaxation data. What should be compared with the τ_c of the bound water is the τ_c of the protein without any contribution from hydration. For the latter, values of 10.2 nsec at 30° and 22.5 nsec at 2° (Table I) can be calculated for the protein with the use of its partial specific volume, 0.751 ml/g, and an asymmetry factor of 1.168⁶¹ to account for the dimer axial ratio of 2:1. These values are in excellent agreement with the experimental τ_c of the bound water at pH 6.2 at 30 and 2° (Table I).

Hydration and dynamics of β -Lg octamer. At pH 4.65, where the protein exists to a large extent as the octamer even at 30° at concentrations above 0.01 g/ml,⁴⁷ the Stokes radius of the bound water is about 30% less than the Stokes radius of the octamer itself. However, this value is

still much closer to the theoretical value than those obtained by other investigators for other proteins.¹⁸⁻²² Furthermore, the 422-symmetry model for the octamer according to Timasheff and Townend⁵⁷ possesses a large central cavity which could accommodate trapped water; if the NMR experiment observed this trapped water, the τ_c value found would be less than that of the protein. Also, if the assumption is made that the NMR hydration of the octamer itself at 2° equals $(\bar{v}'_w)_{\text{pH } 4.65} - (\bar{v}'_w)_{\text{pH } 6.2}$, values from 0.019 to 0.028 g H₂O/g protein can be calculated by the three methods described here. The total volume of the cavity, approximated by an internal sphere tangent to the subunits on the basis of known structural parameters,⁵⁷ amounts to about 6500 Å³. Taking the specific volume of water as unity and thus its molecular volume as 30 Å³/molecule, this would correspond to about 220 mol H₂O/mol of octamer, or 0.027 g H₂O/g protein, which is within range of the NMR-derived hydration values for the octamer.

Since the derived NMR correlation times are number-average values, the hypothesis that the increase in hydration accompanying octamer formation is largely due to trapped water may be tested by calculating a number-average correlation time from the relationship $(\bar{v}_w)_{4.65}\tau_c = (\bar{v}_w)_{6.2}(\tau_c)_0 + [(\bar{v}_w)_{4.65} - (\bar{v}_w)_{6.2}](\tau_c)_{cc}$, where $(\tau_c)_0$ is the correlation time of the octamer at 2° (i.e., 145 nsec, see Table I), $(\tau_c)_{cc}$ is the correlation time of the central cavity of volume 6500 Å³ (i.e., 1.4 nsec), and $(\bar{v}_w)_{6.2}$ and $(\bar{v}_w)_{4.65}$ are the NMR hydration values at pH 6.2 and 4.65, respectively. Calculation of τ_c from ²H NMR hydration values by Method I at 2° gives 36 nsec, in fair agreement with the ²H NMR experimental value of 32.2 ± 4.6 nsec at pH 4.65 and 2°. However, the results of this calculation furnish an indication only of the reasonableness of the approach and not of any exact mechanism of increased hydration accompanying octamer formation.

In contrast to Method I, Method II assumes no constant quadrupole coupling constant and therefore may serve, incidentally, to calculate values of e^2qQ/\hbar (assuming $\eta = 0$) from the \bar{v}'_w values and the relaxation increments obtained by deuterium NMR, together with the experimentally derived τ_c . The quadrupole coupling constants calculated for the respective methods range from 120 to 160 kHz. Hunt and MacKay⁵⁸ have correlated O...D...O and N...D...O hydrogen bond distances with values of quadrupole coupling constants. From their relationships and the above e^2qQ/\hbar values, one obtains distances for O...D...O from 1.5 to 1.7 Å, and for N...D...O from 1.6 to 2.0 Å. These are in agreement with linear hydrogen bond lengths of 1.81 to 1.87 Å recently reported by Ceccarelli *et al.*⁶² in an extensive review of neutron diffraction data.

Contrast of NMR hydration with preferential hydration. To contrast these NMR hydration results with results from another physical method which measures water-protein interactions, preferential hydrations were obtained by Wyman's theory of linked functions,^{28,63} from which it follows that for a tetramerization reaction (dimer \rightarrow octamer, in the case of β -Lg A),

$$\begin{aligned} d \ln k_T / d \ln a_{X,T} &= (\bar{\nu}_{X,T})_{\text{pref}} - 4(\bar{\nu}_{X,M})_{\text{pref}} \\ &= -(W_T/X_T)[(\bar{\nu}_{W,T})_{\text{pref}} - 4(\bar{\nu}_{W,M})_{\text{pref}}] \end{aligned} \quad (19)$$

where the preferential interactions are defined by

$$(\bar{\nu}_X)_{\text{pref}} = \bar{\nu}_X - (X/W)\bar{\nu}_W \text{ and } (\bar{\nu}_W)_{\text{pref}} = \bar{\nu}_W - (W/X)\bar{\nu}_X \quad (19a)$$

Here K_T is the association constant, a_X is the activity of salt, $(\bar{\nu}_{X,T})_{\text{pref}}$ and $(\bar{\nu}_{X,M})_{\text{pref}}$ are the preferential salt binding of octamer (subscript T) and dimer (subscript M), and $(\bar{\nu}_{W,T})_{\text{pref}}$ and $(\bar{\nu}_{W,M})_{\text{pref}}$ are the preferential hydration, respectively. Preferential interaction parameters can thus be readily obtained from the slope of a plot of association constants at various salt concentrations vs the activity of the salt at the corresponding concentrations.

Association constants can be calculated by the use of Gilbert's theory for rapidly reequilibrating association in a sedimenting boundary.^{64,65} Gilbert has shown that for a reversible association there exists a minimum concentration c_{min} above which bimodality of a schlieren ultracentrifuge pattern appears. Furthermore, the area of the slow peak remains constant as the loading concentration is increased well above c_{min} , which is related to the equilibrium constant of the association. Thus, for a tetramerization (in this case, dimer \rightarrow octamer),⁴⁶⁻⁴⁸

$$K_T = M_m^3 \delta [1 + \delta/4(1 - \delta)]^3 / [16(1 - \delta)c^3] \quad (20)$$

where $\delta \equiv (s - s_1)/(s_4 - s_1)$, (s , s_1 , and s_4 being the sedimentation coefficients for the leading edge of the boundary, for the dimer, and for the octamer, respectively), K_T is the association constant, c is the total loading concentration, and M_m is the dimer molecular weight. Since $\delta_{\text{min}} = (n - 2)/3(m - 1)$ and $\delta = 2/9$ for $n = 4$ (where n is the degree of association), $K_1 = 1.087 \times 10^{12}/c_{\text{min}}^3$. The product of the percentage of the slow peak and the loading concentration equals c_{min} , and K_T can thus be evaluated.

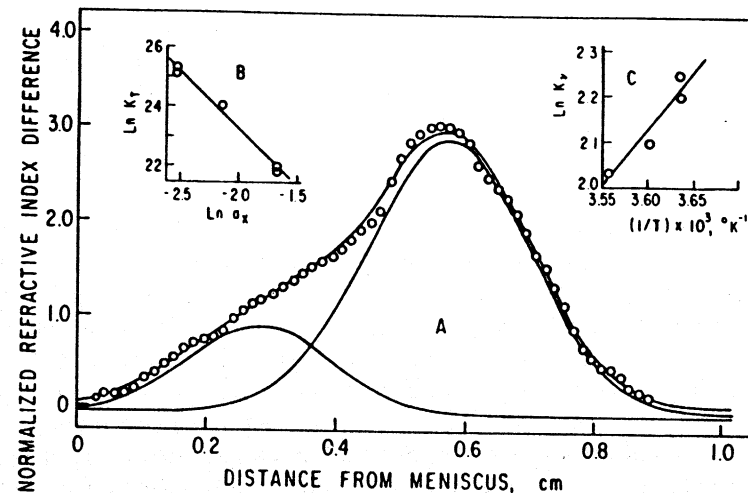


FIG. 5. (A) Sedimentation of β -Lg A under association conditions. Gilbert pattern (open circles) and decomposition into two gaussian peaks (solid lines). (B) Linked-function plot. Plot of logarithm of tetramerization equilibrium constant vs logarithm of activity of salt. The slope is a measure of preferential hydration. (C) van't Hoff plot. Plot of logarithm of equilibrium constant of water binding vs reciprocal of absolute temperature. The slope gives a value of -5.5 ± 1.2 kcal for the enthalpy of hydration. (A, B, and C, taken from Ref. 24.)

In this way, sedimentation velocity data for β -Lg A at pH 4.65 give a linked-function plot (Fig. 5B), which clearly shows a negative slope. From the least-squares value of this slope, a preferential solvation of -3.78 mol salt/mol octamer is calculated. With the assumption that the tetramerization does not release any salt, a value of 0.258 g H_2O /g protein for the preferential hydration is obtained, presumed to be equal to $(\bar{\nu}_W)_{\text{pH 4.65}} - (\bar{\nu}_W)_{\text{pH 6.2}}$ from NMR at 2° . The linked-function preferential hydration thus appears to differ significantly from the NMR hydration difference.

However, as previously noted, NMR probably samples only a certain percentage of the total hydration of a protein. For example, if a major portion of the bound water has a τ_c value of less than 1 nsec, its contributions to the spin-lattice and spin-spin relaxations of the bound state would be equal since at 9.17 MHz the T_1/T_2 ratio for this fast-tumbling water would be unity. Therefore, the correlation time and hydration values calculated from the NMR results by use of a two-state model approximation would yield number-average values weighted toward the slow-tumbling component. It would probably be more realistic to compare the enthalpies of hydration derived by NMR with those from linked functions by the van't Hoff relationship (Fig. 5C). This is possible by assuming a

thermodynamic model involving the transfer of free water to bound water as protein is added to the solution, i.e., $\Delta G = RT \ln(\bar{v}_w/5.56)$. Values of ΔG , ΔH , and ΔS of hydration for each of the three NMR methods are presented in Tables II and III.

From the slope of the van't Hoff plot of Fig. 5C, a ΔH of -5.5 ± 1.2 kcal/mol dimer is obtained. ΔS values calculated at each temperature average -14.1 ± 0.03 eu. The small standard deviation for ΔS indicates constancy of the entropy with respect to temperature and lends support to the model. Furthermore, ΔH of hydration values from NMR range from approximately -6 to -9 kcal/mol dimer, seemingly in agreement, within experimental error, with the value of -5.5 derived from linked functions. Nevertheless, it needs to be remembered that the linked-function method measures the difference between the total hydrations of octamer and dimer, whereas the NMR method yields a quantity proportional to the total hydration of the octamer. Direct comparison of the temperature dependence of these two methods, by assuming that the linked-function hydration is proportional to the difference in the NMR hydration at pH 4.65 and 6.2, is not feasible since the proportionality constant itself should change as a function of temperature. However, the total hydration of the dimer appears to be temperature independent, as indicated by essentially constant NMR hydration values at pH 6.2 for 30 and 2°. These considerations lead to an alternative evaluation of the NMR data in terms of a three-state model.

Isotropic binding, three-state model. For the reasons indicated, an attempt was made to evaluate the ^2H NMR relaxation increment on the basis of a three-state model (i.e., free water, fast-, and slow-tumbling bound water), as used by Cooke and Kuntz in treating lysozyme data,⁶⁶ with the following assumptions. First, the fast-tumbling hydration component of the dimer was assumed to be 0.1 g water/g protein on the following grounds. The lysozyme crystal has been determined to contain 80 molecules of water per protein molecule, or 0.1 g $\text{H}_2\text{O}/\text{g}$ protein,⁶⁷ and 100 to 300 water molecules per crystalline protein molecule distributed over the molecular surface have generally been reported.⁶⁶ For β -Lg, 200 mol water/mol protein is equivalent to 0.1 g water/g protein. Also, Teller *et al.*⁶⁸ have shown that experimentally derived frictional coefficients from sedimentation results are in agreement with those calculated from known X-ray crystallographic structures provided water molecules are added to each charged side chain on the protein surface. The β -Lg dimer has 90

charged amino acids⁶⁹; a value of 0.1 g water/g protein corresponds, therefore, to about two water molecules bound to each charged side-chain amino acid.

Second, since from Teller's work this water would be bound to charged side chains, and since Brown and Pfeffer⁷⁰ have recently shown that deuterium-modified lysine groups tumble at 48 psec, a τ_c value of 48 psec can be assumed. Any water bound to lysine should then have a τ_c value no lower than that of the side chain itself. It was assumed also that, because of the fast segmental motion of the side chain, any increase in association of the protein would not affect this τ_c unless the side chain was directly involved in the interaction site. However, the viscosity and temperature effect on the Stokes-Einstein relationship was taken into account when the temperature changes from 30 to 2°. Finally, the fast-tumbling hydration values at pH 4.65 were increased, by 0.101 at 30° and by 0.258 g $\text{H}_2\text{O}/\text{g}$ protein at 2°, in line with the linked-function results, which indicate such preferential hydrations at these temperatures.

Subtraction of the fast-tumbling contribution from the ^2H NMR spin-lattice and spin-spin relaxation increments yields new values from which the correlation time of the slow component (τ_c)_s and its corresponding hydration (\bar{v}'_w)_s can be calculated. Table IV shows that the (τ_c)_s are slightly larger than the τ_c of Table I, and the (\bar{v}'_w)_s are slightly larger than the \bar{v}'_w of Table II for the two-state model. However, the corresponding values are probably within experimental error, as are the derived enthalpy of hydration of the slow component (Table IV) and the enthalpy of hydration derived from the two-state model (Table II). Calculation of a number-average correlation time of the slow component of the octamer, by assuming that the increase in hydration upon octamer formation is due to water trapped in the cavity of the octamer, yields 37 nsec. This is in reasonable agreement with the experimentally derived value of (τ_c)_s at pH 4.65 and 2° of 42.3 ± 4.6 nsec (Table IV).

Anisotropic binding mechanism. The preceding calculations assume an isotropic relaxation mechanism, as detailed under Theory. In the presence of salt, all the relaxation at pH 6.2 can be accounted for by a slow-tumbling and a fast-tumbling component, amounting to 13 and 204 mol $\text{H}_2\text{O}/\text{mol}$ dimer, respectively, and increasing at pH 4.65 and 2° to 61 and 730 mol $\text{H}_2\text{O}/\text{mol}$ dimer; these may be considered reasonable values for the hydration of a protein.^{1,71}

TABLE IV
TOTAL HYDRATION FOR β -LACTOGLOBULIN DERIVED FROM A THREE-STATE
MODEL (^2H NMR)^{a,b}

pH	T, °C	$(\bar{\nu}'_w)_f$	$(\bar{\nu}'_w)_s$	$(\tau_c)_s$, nsec	$-(\Delta H)_s$, kcal
6.2	30	0.1	0.0054 ± 0.0008	11.0 ± 2.7	0
	2	0.1	0.0056 ± 0.0020	33.9 ± 4.1	
4.65	30	0.201	0.0085 ± 0.0002	28.8 ± 3.3	6.0 ± 1.6
	2	0.358	0.0235 ± 0.0003	42.3 ± 4.6	

^a Assumptions: $(\tau_c)_f = 48$ psec; $(R_{1b})_f = (R_{2b})_f = 31.94$ sec⁻¹ at 30° for pH 6.2 and 4.65; $(R_{1b})_f = (R_{2b})_f = 70.27$ sec⁻¹ at 2° for pH 6.2 and 4.65. Subscripts f and s refer to fast-tumbling and slow-tumbling fractions, respectively.

^b Adapted from Ref. 24.

This does not, however, eliminate the possibility of an anisotropic relaxation mechanism for hydrodynamically bound water. The present results may be interpreted equally well on the basis of the three-component derivation in conjunction with either a two- or three-state model and an appropriate order parameter $S < 1$ [cf. Eqs. (16c,d)]. Here a three-state model is defined, as for the isotropic mechanism (Table IV), as comprising free-motion water, a slow-motion component (i.e., $\tau_c > 5$ nsec), and a fast-motion component (i.e., $\tau_c \cong 48$ psec, as assumed in Table IV). For the latter, under extreme-narrowing conditions the factor S^2 attached to Eqs. (16c,d) is changed to $(1 - S^2)$.²³ The slow motion, in either the two- or three-state anisotropic mechanism, may be due to such processes as protein reorientation, internal motion of the protein, or translational diffusion of water along the protein surface.^{23,32}

Reported values of $S = 0.06$ from ^{17}O relaxation²³ have been obtained by application of line-splitting data for a liquid crystal to a protein, on the assumption that 3 to 6 water molecules are bound to carboxyl groups and 1 to 3 to hydroxyl groups. Theoretical results of Walmsley and Shporer³² give relationships for S (termed the scaling factor by these authors) based on ^1H , ^2H , and ^{17}O relaxation. From these it follows that a value of $S = 0.06$ for ^{17}O would imply $S = 0.12$ for ^2H . At pH 6.2 (30 and 2°) and pH

4.65 (30 and 2°) one obtains [from Eqs. (13a-c) and the ^2H NMR data of Table I for the two-state, and those of Table IV for the three-state model] hydrations of 0.483, 0.500, 0.660, and 2.090 for the two-state, and 0.298, 0.295, 0.509, and 1.250 for the three-state model, respectively. A more reasonable estimate is obtained from the theoretical relationships of Walmsley and Shporer, together with the experimental results of Koenig *et al.*,¹⁸⁻²⁰ which give $S = 0.23$ and corresponding hydrations of 0.119, 0.136, 0.180, 0.569, and 0.102, 0.105, 0.163, 0.435. The ΔH of hydration at pH 4.65 is found to be -6.8 for the two-state and -5.9 kcal for the three-state model. These results agree with the isotropic mechanism (Tables II and IV), since S enters simply as a factor in the Kubo-Tomita-Solomon equations.

Alternatively, equating the preferential hydration from linked functions with the difference between the 2° ^2H NMR hydrations at pH 4.65 and pH 6.2, one obtains $S = 0.30$ for the two-state and $S = 0.26$ for the three-state model, both not far from the 0.23 predicted from the theory of Walmsley and Shporer. Furthermore, with the above values of S the pH 4.65 enthalpies of hydration are -6.8 and -5.9 kcal for the two- and three-state models, respectively. Thus, the increase in hydration as well as the corresponding enthalpy change attendant on octamer formation are the same for either assumption of relaxation mechanism.

The foregoing considerations add up to considerable agreement between certain theoretically and experimentally derived quantities. However, none of the above arguments should be interpreted as proof of any particular NMR mechanism or model, nor of the identity of the particular groups on the protein surface that interact with water. Even without such conclusions, and in place of the quest for absolute values of hydration, it can be useful to scrutinize relative changes in hydration, when these can be taken as functions of changes in secondary, tertiary, or quaternary structure of a protein.

Small-Angle X-Ray Scattering and Velocity Sedimentation

Theory. The theory of SAXS has been presented in some detail in this series by Pessen *et al.*⁶⁰ and by Pilz *et al.*⁷² Elsewhere, with special relevance to the present context, Kumosinski and Pessen^{73,74} have used SAXS results, which implicitly contain the hydration, to calculate sedimentation coefficients without any assumptions concerning the mechanism of hydration. In order to deal with problems of hydration, a multi-

component expression for the chemical potential adapted from Schachman⁴ can be used:

$$\mu_{123} = \mu_2 + (km_1 + \alpha)\mu_1 + km_3\mu_3 \quad (21)$$

Here μ_{123} is the total chemical potential of the sedimenting unit (identical with the fluctuating unit in SAXS), containing component 1 (water), 2 (macromolecule), and 3 (salt); μ_i and m_i ($i = 1, 2, 3$) are the chemical potential and the molality of the respective component; k is a proportionality constant, equal to the ratio of the fraction of salt proportionally bound (proportionally, that is, to the molality of salt in the bulk of the solution) to the molality of the protein; and α is the preferential hydration of the protein, i.e., if positive, the hydration beyond that corresponding to the bulk ratio of water to salt, in moles water bound preferentially per mole protein. It is readily seen that there are $(km_1 + \alpha)$ moles of water and km_3 moles of salt per mole of protein bound to the macromolecule. The term α is related to the preferential salt binding $(\partial m_3/\partial m_2)_\mu$, used in investigations with other experimental techniques, by the expression

$$\alpha = (m_1/m_3)(\partial m_3/\partial m_2)_\mu \quad (21a)$$

Differentiating Eq. (21) with respect to pressure at constant temperature, rearranging, replacing the molal units by concentrations in grams per gram of water, and noting that the partial specific volume of the sedimenting or fluctuating unit, \bar{v}_{123} , can be expressed as $V_{123}N/M_{123}$, yields

$$V_{123}N/M_2 = \bar{v}_2 + (k'g_1 + \xi_1)\bar{v}_1 + k'g_3\bar{v}_3 \quad (22a)$$

Here N is Avogadro's number; M_i , \bar{v}_i , g_i ($i = 1, 2, 3$) are the molecular weight, partial specific volume, and concentration in grams per gram of water of the respective component; $k' = 1000 k/M_2$ equals the amount of salt bound in proportion to its concentration in the bulk of the solution, in grams of component so bound per gram of protein; and $\xi_1 = \alpha M_1/M_2$ is the preferential binding, in grams of water so bound per gram of protein. In 0.1 M salt solution, $g_3 \approx 0.006 \ll 1$, and Eq. (22a) reduces to

$$V_{123}N/M_2 \approx \bar{v}_2 + (k'g_1 + \xi_1)\bar{v}_1 \quad (22b)$$

where g_1 is unity, by definition, and $\bar{v}_1 \approx 1$, since sedimentation coefficients are routinely extrapolated to zero protein concentration.

But the sum of the hydration proportional to bulk concentration, $k'g_1$, and the preferential hydration, ξ_1 , by the definition of the latter, equals the total hydration A_1 [i.e., $\xi_1 \approx A_1 - k'g_1$, see Ref. 27, where A_3/g_3 evidently is identical to our k' ; A_1 is conceptually, though not necessarily experimentally, identical to the \bar{v}'_w of Eq. (13), while V_{123} is the hydrated volume, V , obtained by SAXS]. Thus

$$V_{123}N/M_2 \approx \bar{v}_2 + A_1\bar{v}_1 \quad (22c)$$

and the total hydration is measured by the difference between the hydrated molecular volume and the partial specific volume, in compatible units. The effect of salt binding in this respect is negligible as long as salt concentrations are of the order indicated above. In solutions of high salt concentration, or even moderate concentration when salt binding is strong [i.e., when the preferential salt binding is positive and the preferential hydration in consequence negative; cf. Eq. (21a)], salt will contribute to the solvated volume by way of the third term in Eq. (22a).

As mentioned, it has been shown that, in addition to Stokes radii and frictional coefficients, sedimentation coefficients can be calculated from SAXS data.^{73,75} Differentiating Eq. (21) as before and combining the result with the Svedberg transport equation,⁵ with due regard for the makeup of the sedimenting unit, gives

$$s_{20,w}^0 = \frac{M_2(1 - \bar{v}_2\rho) + \alpha M_1(1 - \bar{v}_1\rho) + km_1M_1(1 - \bar{v}_1\rho) + km_3M_3(1 - \bar{v}_3\rho)}{f_{123}N} \quad (23)$$

where f_{123} is the frictional coefficient of the sedimenting unit, and the other symbols have been defined above. Again, $\bar{v}_1, \rho \approx 1$ and $m_3 \ll 1$, so that all terms beyond the first become negligible and

$$s_{20,2}^0 \approx \frac{M_2(1 - \bar{v}_2\rho)}{f_{123}N} \quad (23a)$$

From this, it may appear at first that the solvation of the protein should have no effect on the sedimentation coefficient. This, however, would be losing sight of the variability of the term f_{123} , which indeed has been commonly neglected in the context of sedimentation coefficients, even though the variability of the analogous term f_{12} has long been acknowledged.^{75,76} As a matter of principle it would, therefore, be an error not to consider this effect here.

The frictional coefficient f_{123} is obtained from

$$f_{123} = (f/f_0)_{123} 6\pi\eta N(r_s)_{123} \quad (24)$$

where $(r_s)_{123}$, the Stokes radius of the sedimenting unit (solvated protein), has traditionally been evaluated from the protein partial specific volume, \bar{v}_2 . The present approach more appropriately uses the hydrated volume,

V , from SAXS, so that $(r_s)_{123}$ equals $(3V/4\pi)^{1/3}$. There are then two terms that depend upon the binding of salt and water to the protein, namely, V_{123} and $(f/f_0)_{123}$. V_{123} is readily related to the hydration by Eq. (22c). The binding contribution to the term $(f/f_0)_{123}$ is not obtained by this method, but it may become possible to compare (f/f_0) evaluated from X-ray diffraction data with the $(f/f_0)_{123}$ from SAXS to find out where the water molecules are located.

Experimental Procedures. Experimental SAXS procedures have been described and discussed in detail in this series^{60,72} and elsewhere.^{73,74}

The technique of sedimentation analysis has been extensively treated by Svedberg and Pederson,⁵ Schachman,⁴ and others. Use of ultraviolet absorption with a photometric scanner interfaced to a computer, besides greatly speeding data collection, facilitates the requisite extrapolation to infinite dilution because it permits sensitive measurements at very low concentrations.⁷⁴

Analysis of Data. In the last column of Table V are listed the values of A_1 calculated from the SAXS volume for 19 globular proteins and 2 spherical viruses.⁷³ Here, the first nine proteins have an average value of 0.280 g H₂O/g protein, in fair accord with generally assumed value of about 0.25 g H₂O/g protein.^{1,3,77} The last 10, which have higher molecular weights (>100,000) and are actually oligomeric structures, average near 0.444 g per g of protein. This higher value might be expected since the phenomenon of trapped solvent (internal solvation) has been observed in such multisubunit structures as casein micelles, viruses, and aspartate transcarbamylase.³

There may also be a dynamic contribution to the hydration, since it is measured by the difference between two volumes. The concept of protein "breathing" has been emphasized before,⁷⁸ and the entire topic of protein dynamics has been reviewed recently.^{79,80} The effects of dynamic changes such as fluctuations (e.g., ring flipping and domain hinge bending) on packing volumes and accessible surface areas remain unclear. Progress on these questions may come from dynamic modeling by computer simulation.

Unless a particle is known to be spherical (e.g., a spherical virus, from electron microscopic evidence), sedimentation analysis by itself can only determine a frictional coefficient which is a combination of a structural and a hydration contribution,^{3,77} and from which, therefore, the structural contribution must be detached in order to get at the hydration. SAXS,

TABLE V
STRUCTURAL AND HYDRODYNAMIC PARAMETERS FROM SAXS^{a,1}

Macromolecule	Model ^b	M^c	Parameters		From V and \bar{v}	
			\bar{v} , ml/g ^d	V , Å ³	A_1 , g/g ^e	\bar{v}
1. Ribonuclease (bovine pancreas) ^{1,2}	PE	13,690 ^f	0.696 ^g	22,000	0.272	
2. Lysozyme (chicken egg white) ²	PE	14,310 ^h	0.702 ^g	24,200	0.317	
3. α -Lactalbumin (bovine milk) ²	PE	14,180 ^h	0.704 ^g	25,100	0.362	
4. α -Chymotrypsin (bovine pancreas) ¹	PE	22,000 ⁱ	0.736	37,170 ^j	0.282	
5. Chymotrypsinogen A (bovine pancreas) ⁵	PE	25,000 ⁱ	0.736	37,790 ^j	0.175	
6. Pepsin ^{h,1}	PE	34,160 ⁷	0.725 ^g	54,870 ^j	0.243	
7. Riboflavin-binding protein, apo (pH 3.0) (chicken egg white) ⁹	PE	32,500 ⁱ	0.720	66,500	0.513	
8. Riboflavin-binding protein, holo (pH 7.0) (chicken egg white) ⁹	PE	32,500 ⁱ	0.720 ^m	55,600	0.311	
9. β -Lactoglobulin A dimer (bovine milk) ¹⁰	PE	36,730 ⁿ	0.751 ^g	60,250 ^o	0.237	
10. Bovine serum albumin ¹¹	PE	66,300 ^p	0.735 ^g	115,940 ^o	0.318	
10a. Lactate dehydrogenase, M ₄ (dogfish) ¹²	OE	138,320	0.741	253,300 ^r	0.362	
11. β -Lactoglobulin A octamer (bovine milk) ¹⁰	OE	146,940	0.751 ^g	215,000 ^o	0.130	
12. Glyceraldhyde-3-phosphate dehydrogenase, apo (bakers' yeast) ¹²	HOC	142,870 ^r	0.737 ¹³	264,200	0.377	
13. Glyceraldhyde-3-phosphate dehydrogenase, holo (bakers' yeast) ¹²	HOC	145,520 ^r	0.737 ^m	250,000	0.298	
14. Malate synthase (bakers' yeast) ¹⁴	OE	170,000 ^r	0.735	338,000	0.463	

(continued)

Macromolecule	Model ^b	M ^c	Parameters		From V and \bar{v}
			\bar{v} , ml/g ^d	V, Å ³	
15. Pyruvate kinase, apo ^e (brewer's yeast) ¹⁵	OEC	190,800 ^a	0.734 ¹⁶	406,000	0.548
16. Pyruvate kinase, holo ^e (brewer's yeast) ¹⁵	OEC	192,160 ^a	0.734 ¹⁶	406,000	0.539
17. Catalase (bovine liver) ¹⁷	PC	248,000 ¹⁸	0.730 ^d	420,000	0.290
18. Glutamate dehydrogenase (bovine liver) ¹⁹	PC	312,000 ²⁰	0.749 ²⁰	668,000	0.541
19. Turnip yellow mosaic virus ²¹	S	4.97 × 10 ⁶ ²²	0.666 ²²	11.49 × 10 ⁶ ^j	0.727
20. Southern bean mosaic virus ²³	S	6.63 × 10 ⁶ ²⁴	0.696 ²⁴	12.25 × 10 ⁶ ^j	0.417

^a Excepted from amended compilation of Ref. 1 of this table. Superscript numbers following entries indicate original references, listed in / below. Tabulated data were taken from the references thus designated in this column, unless noted otherwise for a particular parameter.

^b Geometric model used to describe scattering particle: PE, prolate ellipsoid; OE, oblate ellipsoid; PC, prolate (elongated) cylinder; OEC, oblate (flattened) elliptical cylinder; HOC, hollow oblate cylinder; S, sphere.

^c Molecular weights, by preference, were based on amino acid compositions and sequences wherever available, except in some cases where the cited authors' values appeared more reliable or consistent with other parameters under the conditions of measurement.

^d Partial specific volumes were the cited authors' values or, in some cases, more accurate values found in the literature. Corrections for temperature differences between 25 and 20°C were not in general made for \bar{v} because resulting differences were minimal.

^e From Eq. (9c).

^f From Dayhoff (Ref. 3, this table), p. D-130.

^g From Dayhoff (Ref. 3, this table), p. D-138.

^h From Dayhoff (Ref. 3, this table), p. D-136.

ⁱ Value reported by cited authors (see Note c). For 15, molecular weight calculated from value for subunits by same authors.

^j Secondary parameter, calculated with use of indicated model from values of primary parameters of cited authors.

^k Key to References:

¹ T. F. Kumosinski and H. Pessen, *Arch. Biochem. Biophys.* **219**, 89 (1982).

² H. Pessen, T. F. Kumosinski, and S. N. Timasheff, *J. Agric. Food Chem.* **19**, 698 (1971).

³ M. O. Dayhoff, ed., "Atlas of Protein Sequence and Structure." Vol. 5. Natl. Biomed. Res. Found., Washington, D.C., 1972.

⁴ J. C. Lee and S. N. Timasheff, *Biochemistry* **13**, 257 (1974).

⁵ W. R. Krigbaum and R. W. Godwin, *Biochemistry* **7**, 3126 (1968).

⁶ A. A. Razina, V. V. Lednev, and B. K. Lemzhikin, *Biokhimiya (Moscow)* **31**, 629 (1966).

⁷ T. G. Rajopalan, S. Moore, and W. H. Stein, *J. Biol. Chem.* **241**, 4940 (1966).

⁸ T. L. McMeekin, M. Wilensky, and M. L. Groves, *Biochem. Biophys. Res. Commun.* **7**, 151 (1962).

⁹ T. F. Kumosinski, H. Pessen, and H. M. Farrell, Jr., *Arch. Biochem. Biophys.* **214**, 714 (1982).

¹⁰ J. Witz, S. N. Timasheff, and V. Luzzati, *J. Am. Chem. Soc.* **86**, 168 (1964).

¹¹ V. Luzzati, J. Witz, and A. Nicolai, *J. Mol. Biol.* **3**, 379 (1961).

¹² H. Durchschlag, G. Puchwein, O. Kratky, I. Schuster, and K. Kirschner, *Eur. J. Biochem.* **19**, 9 (1971).

¹³ R. Jaenicke, D. Schmid, and S. Knof, *Biochemistry* **7**, 919 (1968).

¹⁴ D. Zipper and H. Durchschlag, *Eur. J. Biochem.* **87**, 85 (1978).

¹⁵ K. Müller, O. Kratky, P. Röschlau, and B. Hess, *Hoppe-Seyler's Z. Physiol. Chem.* **353**, 803 (1972).

¹⁶ H. Bischofberger, B. Hess, and P. Röschlau, *Hoppe-Seyler's Z. Physiol. Chem.* **352**, 1139 (1971).

¹⁷ A. G. Malmon, *Biochim. Biophys. Acta* **26**, 233 (1957).

¹⁸ J. B. Sumner and N. Gralén, *J. Biol. Chem.* **125**, 33 (1938).

¹⁹ I. Pilz and H. Sund, *Eur. J. Biochem.* **20**, 561 (1971).

²⁰ E. Reisler, J. Pouyet, and H. Eisenberg, *Biochemistry* **9**, 3095 (1970).

²¹ P. W. Schmidt, P. Kaesberg, and W. W. Beeman, *Biochim. Biophys. Acta* **14**, 1 (1954).

²² R. Markham, *Discuss. Faraday Soc.* **11**, 221 (1951).

²³ B. R. Leonard, Jr., J. W. Anderegg, S. Shulman, P. Kaesberg, and W. W. Beeman, *Biochim. Biophys. Acta* **12**, 499 (1953).

²⁴ G. L. Miller and W. C. Price, *Arch. Biochem. Biophys.* **10**, 467 (1946).

^a Value for apoenzyme used, since \bar{v} for holoenzyme not available.

^b From M. O. Dayhoff, ed., "Atlas of Protein Sequence and Structure." Suppl. 1, p. S-83. Natl. Biomed. Res. Found., Washington, D.C., 1973.

^c Unpublished data of authors of Ref. 10, this table (S. N. Timasheff, personal communication).

^d From M. O. Dayhoff, ed., "Atlas of Protein Sequence and Structure." Suppl. 2, p. 267. Natl. Biomed. Res. Found., Washington, D.C., 1976.

^e Molecular volume as well as molecular weight reported by the cited authors appeared to be high, pointing to the possible presence of aggregation products. Values listed are the amino acids sequence molecular weight and a proportionally adjusted molecular volume.

^f Unpublished data of H. Pessen, T. F. Kumosinski, G. S. Fosmire, and S. N. Timasheff.

^g Value for 9 (dimer) used, since \bar{v} for octamer not available.

^h From Dayhoff (Ref. 3, this table), pp. D-147, D-148.

ⁱ Calculated from value for apoenzyme.

^j The designations "apo" and "holo," not strictly correct here, are used for brevity to refer to "native" and "fructose diphosphate liganded," respectively.

^k Molecular weight calculated from value for subunits reported by Bischofberger *et al.* (Ref. 16, this table).

which permits shape analysis, is a means to obtain this structural contribution, making use of known relationships between shape and structural frictional coefficient.^{3,68,73,74,80-82}

This combination of SAXS with sedimentation analysis has been validated for its predictive value by the work of several authors.^{73,75} (See also the chapter "Structural Interpretation of Hydrodynamic Measurements of Proteins in Solution through Correlation with X-Ray Data" in this volume.⁸³) It may be noted that correlations between SAXS and hydrodynamic methods other than sedimentation (viscosity, diffusion), and between various combinations of hydrodynamic data with each other, have been less successful.^{3,68,73}

Discussion of Approaches

The hydrodynamic approach, as pointed out in that section, cannot stand alone. At best, it requires supplementation by a structural method, preferably SAXS, to give unequivocal information on hydration. Furthermore, it has been demonstrated that sedimentation and SAXS information can be correlated to the extent that sedimentation parameters are fairly predictable^{73,75} and, in effect, do not constitute an independent method. It would appear, then, that for the purpose of investigating hydration, SAXS could be considered a more useful approach than sedimentation, and that it might replace the latter, were it not for the circumstance that, in contemporary laboratories, SAXS instruments are even rarer than analytical ultracentrifuges.

The SAXS method, for practical purposes, suffers from the lack of a substantial published data base. It would be helpful if investigators reporting SAXS results on a protein undertook the labor of calculating and disseminating a full set of the parameters their data are capable of generating⁷⁴ instead of merely those engaging their immediate attention. Further, it is to be hoped that larger numbers of those interested in hydration and structural information will be enabled to use this powerful and versatile method which, with the commercial availability in recent years of position-sensitive detectors, has been a very productive method as well.

In lieu of SAXS data, NMR is capable of giving information on hydration. Absolute values of NMR hydration are not completely independent of assumptions regarding mechanism, whereas relative values are largely independent of such assumptions and can serve to assess changes in structure or biochemical behavior as a function of varying environmental

conditions. The interpretation of such changes of course will depend on the system studied.

One way of using NMR relaxation to obtain this kind of information has been by means of frequency dependence.²⁰ There are, however, few instruments available that allow dispersive measurements. Attention must be paid to the frequencies chosen: if measurements are made at two different frequencies to eliminate one of the modes of relaxation used here [cf. Eqs. (16a) and (16b)], care must be taken that the frequencies are sufficiently different to exhibit a substantial enough dispersion for adequate relaxation statistics. In any case, the frequencies must be high enough (and so must the molecular weight, on which the correlation time depends) to escape the line-narrowing region, i.e., $\omega_0^2 \tau_c^2$ must be distinctly larger than 1. Otherwise, the appropriate simultaneous equations will either have no solution, or the solution will be very imprecise.

In place of frequency dependence, concentration dependence (accessible with any NMR instrument) has been emphasized here. Two modes of relaxation, spin-lattice and spin-spin, were used with deuteron resonance to avoid the cross-relaxation encountered with spin-lattice relaxation of protons. ¹⁷O relaxation has also been used, for similar reasons.^{19,23} In a different method, proton spin-lattice relaxation has been employed, but cross-relaxation effects were determined and allowed for by the joint examination of two genetic variants of the same protein, which differed only in the known extent of an association reaction.²⁵ Again, the combination of protein molecular weight and resonant frequency must satisfy the condition for avoiding the line-narrowing mentioned.

In addition to hydration, NMR relaxation gives other valuable information that can be correlated with structural and biochemical changes. Correlation times, obtained from Eqs. (16a) and (16b), are related to molecular size and shape and are relevant to hydrodynamics. Virial coefficients, for which concentration dependence data are indispensable, can be evaluated directly from a concentration plot. From Eq. (13c), in light of the discussion of Fig. 2, it follows for either mode of relaxation that $R = \bar{v}'_w(R_b - R_f)c \exp(2B_0c) + R_f$. It can be seen that nonlinear regression applied to this relationship gives the virial coefficient B_0 directly. The data of Fig. 2 gave $B_0 = 8.22$ ml/g, which is in close agreement with the literature value of 8.5 ml/g, obtained from light scattering.⁴⁵ Virial coefficients, related to the average net charge carried by molecules, provide a particularly useful measure of molecular interaction.